Research Article | Vol. 26, No. 7 | 2 Apr 2018 | OPTICS EXPRESS 8470
Optics EXPRESS

Optimizing band-edge slow light in silicon-on-insulator waveguide gratings

MARCO PASSONI,[1] DARIO GERACE,[1] LIAM O'FAOLAIN,[2,3] AND LUCIO CLAUDIO ANDREANI[1,*]

[1]*Department of Physics and CNISM, University of Pavia, 27100 Pavia, Italy*
[2]*Centre for Advanced Photonics and Process Analysis, Cork Institute of Technology, Cork, Ireland*
[3]*Tyndall National Institute, Cork, Ireland*
[*]*lucio.andreani@unipv.it*

Abstract: A systematic analysis of photonic bands and group index in silicon grating waveguides is performed, in order to optimize band-edge slow-light behavior in integrated structures with low losses. A combination of numerical methods and perturbation theory is adopted. It is shown that a substantial increase of slow light bandwidth is achieved when decreasing the internal width of the waveguide and the silicon thickness in the cladding region. It is also observed that a reduction of the internal width does not undermine the performance of an adiabatic taper.

OCIS codes: (050.5298) Photonic crystals; (130.2790) Guided waves; (250.5300) Photonic integrated circuits.

References and links

1. T. F. Krauss, "Why do we need slow light?" Nat. Photonics **2**, 448–450 (2008).
2. T. Baba, "Slow light in photonic crystals," Nat. Photonics **2**, 465–473 (2008).
3. R. S. Tucker, P.-C. Ku, and C. J. Chang-Hasnain, "Slow-light optical buffers: capabilities and fundamental limitations," J. Light. Technol. **23**, 4046–4066 (2005).
4. H. C. Nguyen, S. Hashimoto, M. Shinkawa, and T. Baba, "Compact and fast photonic crystal silicon optical modulators," Opt. Express **20**, 22465–22474 (2012).
5. A. Brimont, D. Thomson, F. Gardes, J. Fedeli, G. Reed, J. Martí, and P. Sanchis, "High-contrast 40 gb/s operation of a 500 μm long silicon carrier-depletion slow wave modulator," Opt. Lett. **37**, 3504–3506 (2012).
6. Z. Shi, R. W. Boyd, D. J. Gauthier, and C. Dudley, "Enhancing the spectral sensitivity of interferometers using slow-light media," Opt. Lett. **32**, 915–917 (2007).
7. K. Qin, S. Hu, S. T. Retterer, I. I. Kravchenko, and S. M. Weiss, "Slow light mach–zehnder interferometer as label-free biosensor with scalable sensitivity," Opt. letters **41**, 753–756 (2016).
8. A. Canciamilla, M. Torregiani, C. Ferrari, F. Morichetti, R. De La Rue, A. Samarelli, M. Sorel, and A. Melloni, "Silicon coupled-ring resonator structures for slow light applications: potential, impairments and ultimate limits," J. Opt. **12**, 104008 (2010).
9. M. Minkov and V. Savona, "Wide-band slow light in compact photonic crystal coupled-cavity waveguides," Optica. **2**, 631–634 (2015).
10. J. Li, T. P. White, L. O'Faolain, A. Gomez-Iglesias, and T. F. Krauss, "Systematic design of flat band slow light in photonic crystal waveguides," Opt. Express **16**, 6227–6232 (2008).
11. M. F. Yanik, W. Suh, Z. Wang, and S. Fan, "Stopping light in a waveguide with an all-optical analog of electromagnetically induced transparency," Phys. Rev. Lett. **93**, 233903 (2004).
12. M. Scalora, R. Flynn, S. Reinhardt, R. Fork, M. Bloemer, M. Tocci, C. Bowden, H. Ledbetter, J. Bendickson, J. Dowling *et al.*, "Ultrashort pulse propagation at the photonic band edge: Large tunable group delay with minimal distortion and loss," Phys. Rev. E **54**, R1078 (1996).
13. D. Gerace and L. C. Andreani, "Gap maps and intrinsic diffraction losses in one-dimensional photonic crystal slabs," Phys. Rev. E **69**, 056603 (2004).
14. M. Povinelli, S. G. Johnson, and J. Joannopoulos, "Slow-light, band-edge waveguides for tunable time delays," Opt. Express **13**, 7145–7159 (2005).
15. C. Sciancalepore, K. Hassan, T. Ferrotti, J. Harduin, H. Duprez, S. Menezo, and B. B. Bakir, "Low-loss adiabatically-tapered high-contrast gratings for slow-wave modulators on soi," Proc. SPIE **9372**, 93720G (2015).
16. G. T. Reed, G. Mashanovich, F. Gardes, and D. Thomson, "Silicon optical modulators," Nat. Photonics **4**, 518–526 (2010).
17. L. Li, "Formulation and comparison of two recursive matrix algorithms for modeling layered diffraction gratings," J. Opt. Soc. Am. A **13**, 1024–1035 (1996).
18. L. Li, "New formulation of the fourier modal method for crossed surface-relief gratings," J. Opt. Soc. Am. A **14**, 2758–2767 (1997).

#315253 https://doi.org/10.1364/OE.26.008470
Journal © 2018 Received 12 Dec 2017; revised 15 Feb 2018; accepted 15 Feb 2018; published 23 Mar 2018

Optics EXPRESS

19. J. Hugonin, P. Lalanne, I. D. Villar, and I. Matias, "Fourier modal methods for modeling optical dielectric waveguides," Opt. Quantum Electron. **37**, 107–119 (2005).

1. Introduction

Slow light in Photonic Integrated Circuits (PICs), especially in the field of Silicon Photonics, has drawn considerable attention in recent years because of the fundamental interest in controlling how light propagates, and thanks to the advanced functionalities and improved performance that are provided by a long interaction time in the medium [1, 2]. In fact, slow light can provide enhancement of light-matter interaction in a way similar to optical resonators, but retaining the large bandwidth of traveling wave devices. Example applications are the realization of all-optical buffers and memories [3], or the enhancement in sensitivity of interferometers, for example in Mach-Zehnder modulators [4, 5] or for sensing purposes [6, 7].

Various approaches to slow down light in PICs have been studied. The most common ones are based either on coupled cavities, usually rings [8] or Photonic Crystal (PhC) resonators [9], or on PhC waveguides with tailored dispersion [10], or on all-optical analogs of EIT [11]. These approaches lead to a very low group velocity and/or a relatively wide bandwidth with low Group Velocity Dispersion (GVD). The realisation of a large bandwidth together with low GVD requires the photonic dispersion to be almost linear in the spectral region of interest. This is a desirable feature but usually requires a complex design leading to substantial propagation and insertion losses.

In this work, we focus on the conceptually simpler approach of band-edge slow light in one-dimensional periodic structures. This follows naturally from the fact that the dispersion of light in a periodic structure is flat near the photonic band gap [12, 13]. Band-edge slow light can be implemented in PICs by using Grating Waveguides [14], namely conventional ridge waveguides with a periodic modulation of their width. The advantage of such structures is that they are easy to produce with the fabrication techniques for silicon based PICs, propagation losses are low as they operate below the cladding light line, and insertion losses can be reduced to very small values by the application of adiabatic taper [15].

Furthermore, electro-optic modulation is a key function in optical communication systems. Such devices require invariably to realize electrical contacts to the waveguide, which makes the rib waveguide structure one of the most commonly used systems [16]. The low refractive index contrast inherent with such an approach places a serious physical constraint on the performance of slow light devices. Nonetheless, reducing the footprint of optical modulators is a crucial goal for the field of silicon photonics, therefore giving band-edge slow light in rib waveguides considerable practical importance [15].

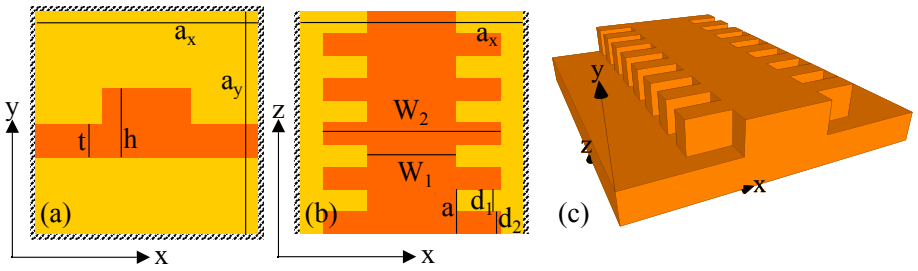

Fig. 1. Schematic cross section (a), top view (b) and 3D view (c) of the grating waveguide structure analyzed in this work. All the relevant parameters are defined: orange represents Si and yellow represents SiO_2 materials (missing in 3D view). The black banded region in the 2D view shows the borders to which coordinate transformations are applied (see Sec. 2).

Optics EXPRESS

The aim of this work is to optimize the performance of band-edge slow light in general, and for rib waveguide structures in particular (see Fig. 1). We calculate the photonic dispersion by combining a numerical approach (aperiodic-Fourier Modal Method) and Perturbation Theory, which allows us to examine a large parameter space. The maximum slow-light bandwidth occurs when the internal waveguide width goes to zero i.e., for a 1D lattice of trenches, which is problematic for efficient coupling. Realising very low insertion losses by means of tapering is important and a region of parameters is identified where the structure is still a grating waveguide amenable to tapering, and the slow-light bandwidth is close to the maximum values. The results will allow the implementation of slow light in rib-waveguide based devices, such as Mach-Zehnder modulators, reducing their length and thus their power dissipation while maintaining useful bandwidth.

2. Bands calculation and fitting procedure

The numerical analysis presented in this work is carried out using a Python based implementation of the aperiodic Fourier Modal Method (a-FMM), which has proven to be both reliable and fast to deal with such problems. This method combines a 2D Fourier expansion in the xy plane with the scattering matrix algorithm in the z direction [17, 18]. The strength of this method is the possibility to apply a particular coordinate transformation that maps the 2D unit cell of the Fourier expansion to the whole $\mathbb{R}^2$, thus making crosstalk between adjacent replicas of the structure negligible [19]. This allows the application of a class of Fourier Methods to structures that do not exhibit a periodicity in a 2D plane, such as waveguide gratings.

Direct calculation of the complete band structure requires a great number of frequency points (an example is given in Fig. 2(a)), especially in the slow light region where the bands are almost flat. We are interested in the lowest-lying band near the lower gap edge, which minimizes propagation losses in actual experiments. This allows us to reduce the computational effort by using a hybrid approach: perturbation theory is employed to get an analytic expression for the dispersion, depending on a few free parameters, then the numerically calculated dispersion is fitted at a few energy points (≈ 10 per structure) to extract the analytic parameters.

The analytic formula for the fit of the dispersion, which generalizes the quadratic model of Ref. [14], is obtained by perturbing free space propagation through a dielectric constant variation $\Delta\varepsilon$ with a single Fourier component (i.e., the optical analog of the nearly-free electron model in solid state physics). Near the edge of the Brillouin zone the dimensionless frequency

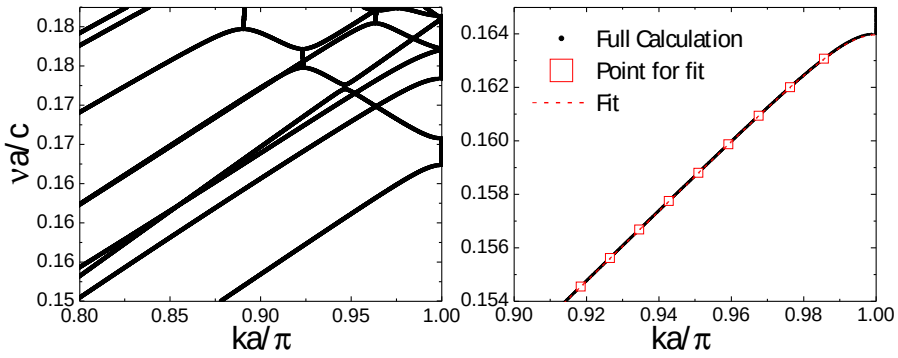

Fig. 2. (a) Complete band dispersion calculated for the same structure as in Ref. [15]; (b) Close-up of the fundamental TE mode near the band gap. Both full numerical solution and the corresponding fit using only the red square points are shown. Parameters of the structure are: W_1 = 400 nm, W_2 = 800 nm, t = 150 nm, a= 213.2 nm, d_2/a=0.5; Fit parameters are: $\Omega_0 = 1.6559 \cdot 10^{-1}$, $n = 3.3429$, $U = 2.3945 \cdot 10^{-2}$.

Optics EXPRESS

$\Omega = \nu a/c$ can be expressed as:

$$\Omega(\delta, \Omega_0, n, U) = \left\{ \Omega_0^2 + \left[\delta^2 + \sqrt{\frac{4\delta^2 - \left(1-\delta^2\right)^2 U^2}{4n^2}} \right] \right\}^{\frac{1}{2}} \quad (1)$$

where $\delta = 1 - ka/\pi$. A comparison between this fitting procedure and a direct calculation with several energy points is presented in Fig. 2(b), showing that this method allows calculating the slow light band edge dispersion with high precision, while reducing the computational effort and providing a compact representation of the data.

3. Results

First, we address the study of the band-edge slow light effect as a function of the waveguide geometry, starting from horizontal parameters since the vertical structure is usually fixed by the PIC fabrication technology used (here we choose h=310 nm and t=150 nm, a common platform). All the materials are modeled as lossless dielectrics with $\varepsilon = 12.30$ (Si) and $\varepsilon = 2.09$ (SiO_2). The band dispersion is calculated as a function of W_1, W_2. The period of each structure is chosen to tune the position of the band edge exactly at the target wavelength of λ =1.3 μm. An example of bands calculated for different W_1 values is presented in Fig. 3, where the fundamental mode dispersion is plotted next to its corresponding group index. When decreasing W_1 at fixed other parameters, the bands tend to become flatter and the group index at fixed wavelength increases.

The use of an optimization strategy requires the definition of one or more figures of merit (FoM) that capture the efficiency of slow light behavior of the waveguides allowing a quick comparison between different structures. Inspired by the trend in group index, which increases monotonically towards the band gap before diverging, we choose to define the bandwidth in which the group index is larger than a given cut-off value as the relevant FoM for our purposes. As an example, in Fig. 4 we show a contour plot of the slow light bandwidth for $n_g > 20$, as a function of W_1 and W_2 at fixed d_2/a=0.5. As a first comment, we notice that the largest value of slow light bandwidth is quite small in this case, below 1 nm. Hence, grating waveguides can allow for very large group indices but only within a rather narrow bandwidth (and with very high GVD). As a consequence, the best application of such structures is likely to occur for a lower group index, around 10-15, which allows for a larger bandwidth and lower GVD (as seen in Fig. 6(a), where a plot analogous to Fig. 4 is reported for $n_g > 10$). As a second comment, it is worth stressing that the slow light bandwidth exhibits a quite simple trend: it increases monotonically on decreasing W_1 and increasing W_2.

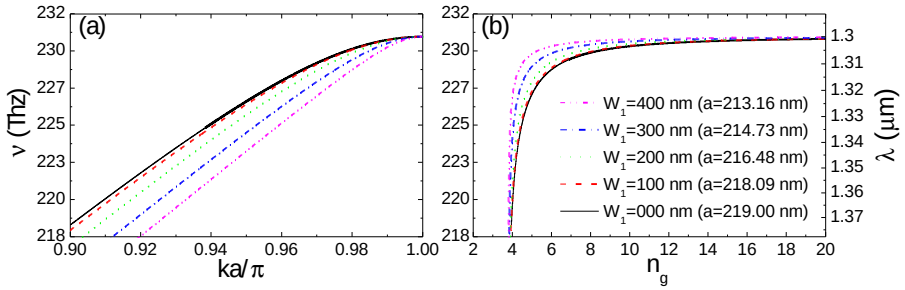

Fig. 3. (a) Band structure and (b) corresponding group index for different widths of the internal section, W_1, (the corresponding period is given in the legend). Fixed parameters are: h = 310 nm, t = 150 nm, W_2 = 800 nm, d_2/a=0.5.

Optics EXPRESS

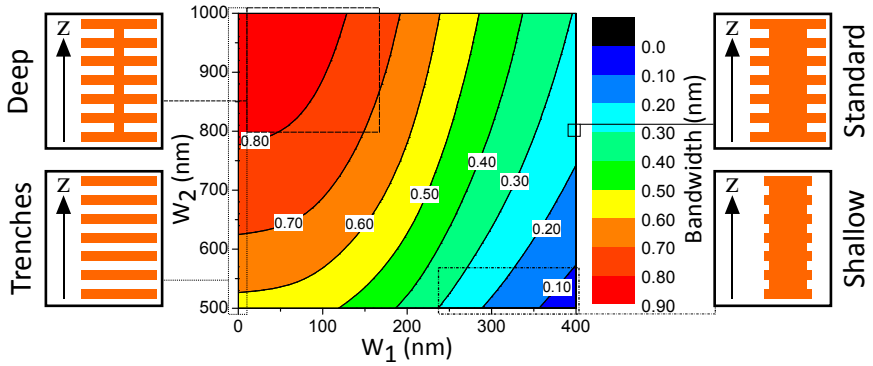

Fig. 4. Contour plot showing the slow light bandwidth for $n_g > 20$ as a function of W_1 and W_2. The other parameters are fixed as $h = 310$ nm, $t = 150$ nm, d_2/a=0.5.

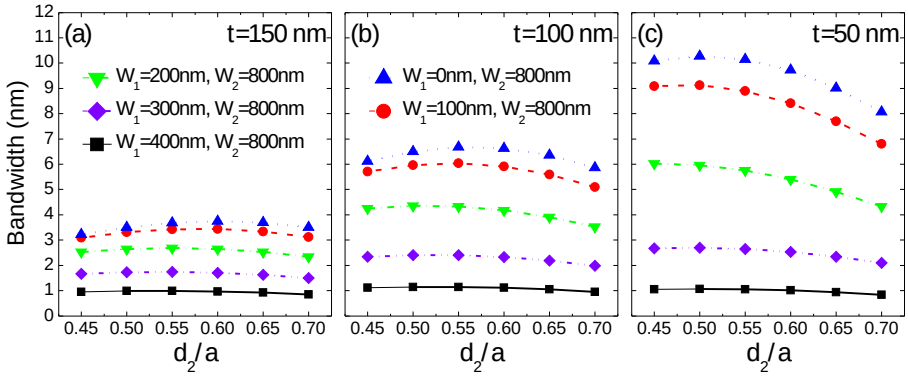

Fig. 5. Slow light bandwidth for $n_g > 10$ as a function of the ratio d_2/a for some selected sets of parameters.

The best structures in terms of slow light bandwidth are the ones in which W_1 goes to zero, i.e., the system reduces to a 1D lattice of trenches. This result is interesting on its own, however it may lead to a critical issue for application requiring low insertion losses of light entering the device. In fact, direct butt coupling of grating waveguides to standard ridges usually causes quite high reflection or scattering losses. This problem is usually solved by adiabatic tapering, which gradually modifies the geometry between the two waveguides allowing for a gradual adjustment of wavevector and mode profile, leading to a strong reduction of such insertion losses. When considering current lithographic techniques, which have some minimum critical dimension, it turns out that an adiabatic taper from ridge waveguide to the lattice of trenches is not a technologically viable route. A solution to this problem can come from using a deep grating waveguide, where W_1 is chosen to be small but compatible with fabrication techniques (i.e., $\approx$ 100 nm); the resulting bandwidth would only be slightly smaller as compared to the lattice of trenches, however this structure could ultimately be tapered, as we show in the next Section.

To further extend our analysis, we now allow for variation of other parameters, in particular of the ratio d_2/a and of the silicon layer thickness in the cladding region surrounding the waveguide, i.e., the parameter t in Fig. 1(a).

The slow light behavior as a function of the ratio d_2/a was analyzed in the range between 0.45 and 0.70 with a 0.05 increment. Some of the results obtained are presented in Fig. 5, where the slow light bandwidth for a group index $n_g > 10$ is explicitly shown for few selected structures. It

Optics EXPRESS

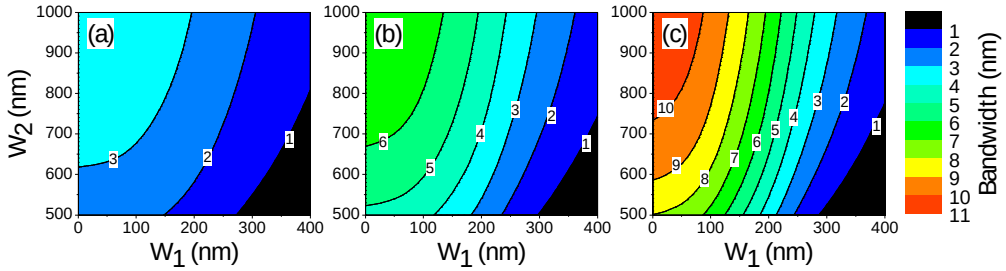

Fig. 6. Contour plot showing the slow light bandwidth for $n_g > 10$ as a function of W_1 and W_2 for $d_2/a = 0.5$ and different values of t: (a) 150 nm, (b) 100 nm, and (c) 50 nm.

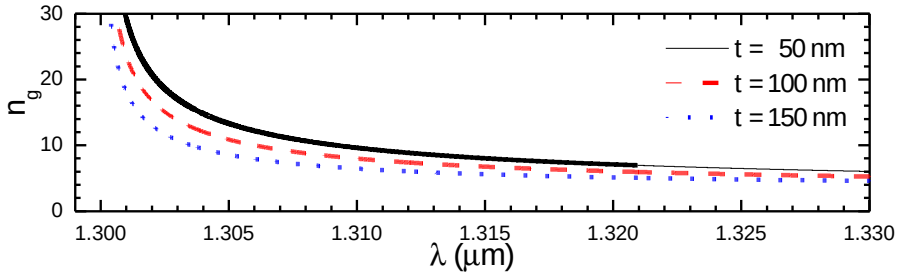

Fig. 7. Evolution of the group index versus wavelength as function of the cladding silicon thickness, t, for the structure with $W_1 = 100$ nm, $W_2 = 800$ nm and $d_2/a = 0.5$. A bandwidth of about 10 nm for $n_g > 10$ is evident for the simulated structure with $t = 50$ nm.

is evident that the variation of the ratio d_2/a around 0.5 weakly affects the overall performance. It is also evident that each structure exhibits a maximum of slow light bandwidth as a function of d_2/a, which is always within the range between 0.45 and 0.6. Values of d_2/a farther from 0.5 are less interesting since such structures would be very difficult to fabricate, requiring proportionally smaller features, and would fall outside the optimal region of parameters. For the rest of this work we will focus on a ratio $d_2/a = 0.5$, as it is the best compromise between performances and possibility of fabrication.

The behavior as a function of the silicon thickness in the cladding region, t, is much more significant. In Figs. 5, 6 and 7 we show that decreasing the thickness t to 100 or 50 nm allows increasing the bandwidth up to 6 or 10 nm, respectively. This is physically explained, since decreasing t increases the effective index contrast between the thin and thick sections of the waveguide. Allowing for full etching of the Si layer would likely boost the performances even further, although it would undermine some targeted applications such as, e.g., electrically driven Mach-Zehnder modulators. Thus, we believe the thickness $t = 50$ nm to be the optimal choice for maximizing slow-light bandwidth while allowing modulation. For details on all the 37 638 analyzed structures see Data File 1 in supplementary material, where the period and fit parameters are reported for each simulated structure.

4. Taper

We now show that reducing W_1 is compatible with the realization of an adiabatic taper. Here we take advantage of the versatility of the a-FMM, which allows to calculate the in-plane transmission and reflection through an arbitrary structure of finite length. As a target structure we consider a finite size grating waveguide with $t = 150$ nm and $W_2 = 800$ nm, coupled at both ends to

Optics EXPRESS

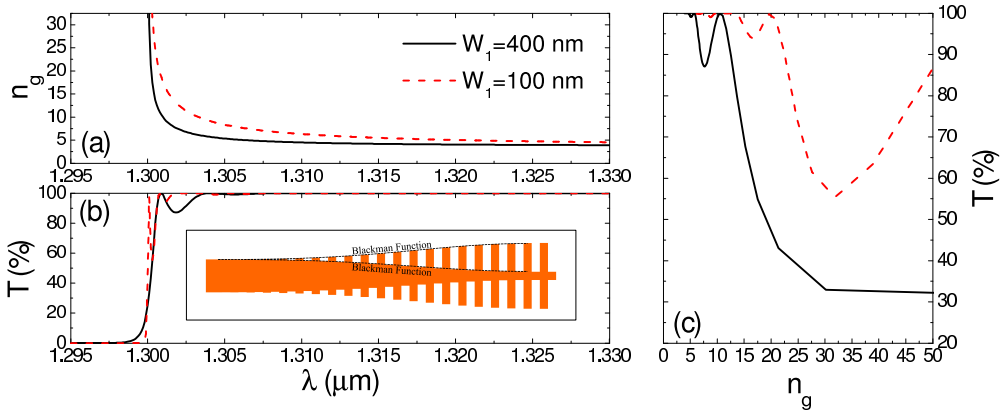

Fig. 8. Performances of 150 periods long adiabatic tapers for t = 150 nm, W_2 = 800 nm and different values of W_1, respectively 100 and 400 nm: (a) group index as a function of wavelength, (b) transmission as a function of wavelength, (c) transmission as a function of group index. An example of a 20 periods long tapering structure is shown in the inset.

a conventional ridge waveguide (400 nm wide) by means of two tapering sections. We have simulated the transmission for different lengths of the slow light region and the tapers. The taper sections are constructed in analogy with Ref. [15], by gradually modulating W_1 and W_2 from the 400 nm width in the ridge waveguide to their respective values in the slow light region with a Blackman function (see, e.g., the inset in Fig. 8(b)). The transmission spectrum typically shows very rapid oscillations that mainly depend on the length of the slow light section (compatible with Fabry-Perot interference in the whole structure), with an overall envelope mainly depending on the taper length.

The transmission through a 128 periods section of a slow light waveguide surrounded by two 150 periods long tapers for two different values of W_1 is shown in Fig. 8. It can be noticed that a relatively short taper ($\approx 30\,\mu$m) is enough to achieve high transmission ($> 90\%$) in almost all the region of interest. Figure 8(c) shows that the W_1 = 100 nm structure keeps a transmission of almost 100% up to a group index of around 20. Thus, reducing W_1 from 400 nm to 100 does not worsen the performances of the taper. This confirms that the structures with W_1 around 100 nm represent an optimal compromise between the requirements of maximizing the slow light bandwidth and having a structure that can be connected to a standard Si waveguide by an adiabatic taper.

5. Application to asymmetric Mach-Zehnder interferometer

To further prove the accuracy and versatility of our method, we decided to tackle the simulation of an actual device. We simulate an asymmetric Mach-Zehnder interferometer similar to the one employed in [15] to demonstrate the slow light effect. The schematic of the interferometer is presented in Fig. 9(a), and it is substantially a conventional Mach-Zehnder interferometer in which the two arms are respectively composed of a ridge waveguide and of a grating waveguide. Standard Multi Mode Interferometers (MMI) or Co-Directional Couplers can be used as beam splitters.

The simulation is based on a simplified 4×4 Scattering Matrix approach (2 channels, forward and backward propagation). To simulate the entire structure we only need two different 4×4 matrices: the one expressing the beam splitters and the one expressing the propagation in the waveguides inside the interferometer.

For the present simulation we assume ideally lossless 50/50 beam splitters, which are

Optics EXPRESS

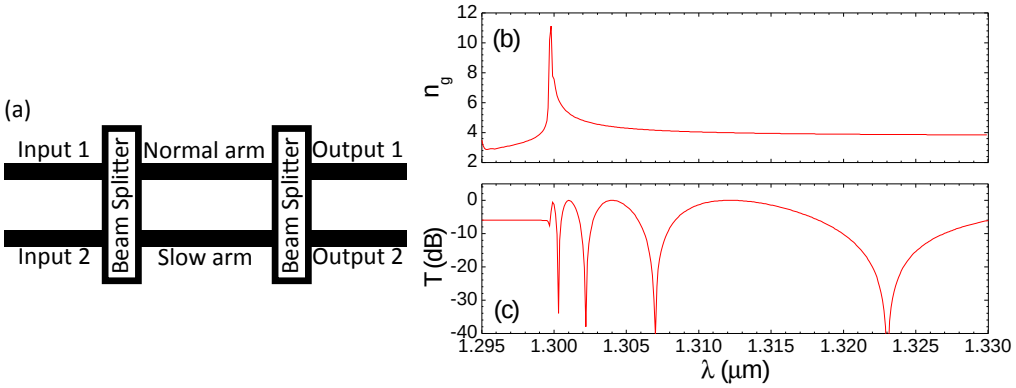

Fig. 9. (a) Schematic representation of the Mach-Zehnder interferometer, (b) effective group index of the slow light arm and (c) transmission at the output 1 channel of the interferometer.

represented by the following scattering matrix:

$$S_{BS} = \frac{1}{\sqrt{2}} \begin{bmatrix} 1 & 1 & 0 & 0 \\ 1 & -1 & 0 & 0 \\ 0 & 0 & 1 & 1 \\ 0 & 0 & 1 & -1 \end{bmatrix} \tag{2}$$

While this approximation is generally a good one, since Co-Directional Couplers and MMI can be realized with very low losses, we have to point out that the extension of this kind of approach to real beam splitters requires only minor modifications to the matrix of Eq. (2).

The propagation scattering matrix is constructed from two 2×2 scattering matrices, expressing the propagation in the normal and slow light waveguides, respectively. The scattering matrix for the propagation in the normal part of the waveguide is easily obtained, first employing the mode solver embedded in the A-FMM to get the dispersion $k = k(\omega)$ of the fundamental mode in the waveguide, and then building the scattering matrix simply as:

$$S_W(\omega) = \begin{bmatrix} e^{ikL} & 0 \\ 0 & e^{ikL} \end{bmatrix} \tag{3}$$

where L is the length of the waveguide.

The propagation matrix of the slow light waveguide can be calculated in two ways. The first is basically the same procedure used in the conventional waveguide but taking the dispersion of the fundamental Bloch mode in the grating. This approach can only model a finite length of periodic waveguide and completely discards the problem of the coupling, but it is simple and computationally mild. The second one consists in modeling a complete finite structure by full calculation with A-FMM (as in the previous section) and then retaining only the elements of the entire scattering matrix between the fundamental input and output modes. This approach is exact and can really simulate existing structures, considering transmission, reflection and losses, but with the drawback of being computationally very expensive.

This second method lends itself also to the calculation of the effective group index of the complete structure, which is simple for a periodic waveguide, but can be trickier when the structure involves tapers or more complicated geometries. To do this we recall that the effective wavevector k can be related to the phase shift ϕ along a distance L by $\phi = kL$. In a scattering matrix calculation we can obtain ϕ by taking the phase of transmission amplitude and then get the group index as:

$$n_g = c\frac{\partial k}{\partial \omega} = \frac{c}{L}\frac{\partial \phi}{\partial \omega} \tag{4}$$

Optics EXPRESS

We apply this framework to the simulation of an asymmetric Mach-Zehnder interferometer, in which the normal arm is composed by a 600 μm conventional ridge waveguide (h = 310 nm, t = 150 nm, W = 400 nm) and the slow light arm is composed by a 100 μm of grating waveguide (W_1 = 400 nm, W_2 = 800 nm, a = 213 nm) between two 250 μm long adiabatic tapers (build as in the previous section). Results are summarized in Figs. 9(b) and 9(c), where the group index calculated with Eq. (4) and the transmission in one of the output channels of the interferometer are shown, respectively. We see that we have a decreasing of the dip spacing when increasing the group index, demonstrating the slow light effect and in agreement with the results reported in Ref. [15] . This type of analysis, which allow us to simulate complete devices and to access quantities that can easily be compared with experiments, can in principle be extended to other structures, such as slow-light based electro-optical modulators.

6. Conclusion

We have analyzed slow light performances of silicon grating waveguides as a function of geometric parameters. The maximum slow-light bandwidth is obtained when the internal waveguide width W_1 is reduced to zero, i.e., for the 1D lattice of trenches. Moreover, the bandwidth is substantially increased (from ~ 3 nm to ~ 10 nm for $n_g > 10$) by reducing the cladding silicon thickness from 150 to 50 nm. While the lattice of trenches cannot be easily connected to a standard Si waveguide with a taper section, group index values that are close to the maximum ones can be obtained with an internal width W_1 of the order of 100 nm. Grating waveguides with such a value of W_1 can be connected to a Si waveguide by a standard adiabatic taper. Transmission through a finite length section of slow light waveguide surrounded by 30 μm long tapers is close to 100% for group indices $n_g < 20$. Applications of such devices should be considered when a moderate increase of group index is required while keeping a simple waveguide structure and retaining very low loss level, as an example in integrated Mach-Zehnder modulators.

Funding

European Union Horizon H2020 Programme (H2020-ICT27-2015, COSMICC n° 688516).

Acknowledgments

We acknowledge the CINECA award under the ISCRA initiative, for the availability of high performance computing resources and support. Useful discussions with A. Fincato, A. Ghilioni, P. Orlandi, F. Svelto are gratefully acknowledged.